drones

MDPI

Article

Energy-Efficient Joint User Association, Backhaul Bandwidth Allocation, and Power Allocation in Cell-Free mmWave UAV Networks

Zhiwei Si [1,*], Zheng Jiang [1], Kaisa Zhang [2], Qian Liu [3,*], Jianchi Zhu [1], Xiaoming She [1] and Peng Chen [1]

[1] 6G Research Centre, China Telecom Beijing Research Institute, Beijing 102209, China; jiangzheng@chinatelecom.cn (Z.J.); zhujc@chinatelecom.cn (J.Z.); shexm@chinatelecom.cn (X.S.); chenpeng11@chinatelecom.cn (P.C.)
[2] School of Electronic Engineering, Beijing University of Posts and Telecommunications, Beijing 100876, China; kaisa@bupt.edu.cn
[3] School of Communication and Information Engineering, Chongqing University of Posts and Telecommunications, Chongqing 400065, China
* Correspondence: sizw@chinatelecom.cn (Z.S.); qianliu@cqupt.edu.cn (Q.L.)

Abstract: In this article, we propose a cell-free network architecture for an unmanned aerial vehicle (UAV) base station (BS), i.e., UBS, incorporating high-altitude platform stations (HAPSs) as central processing units (CPUs). The goal is to guarantee the quality of service (QoS) of user equipment (UE), reduce energy consumption, extend communication time, and facilitate rescue operations. The millimeter-wave (mmWave) frequency band is deployed in access and backhaul links to satisfy UE QoS requirements and high backhaul demands. The proposed framework jointly optimizes user association, backhaul bandwidth allocation, and power allocation to maximize energy efficiency while meeting QoS requirements. The optimization problem, modeled as non-convex mixed-integer nonlinear fractional programming, is solved through a three-stage iterative algorithm. This includes (1) optimizing power allocation based on Dinkelbach transformation and a successive convex approximation (SCA) method, (2) clustering UBSs using the Lagrangian method, and (3) deriving a closed-form bandwidth allocation factor. The proposed algorithm significantly outperforms many traditional algorithms in performance while maintaining low computational complexity.

Keywords: unmanned aerial vehicle (UAV); millimeter-wave; high-altitude platform station (HAPS); central processing unit (CPU)

Academic Editor: Rosdiadee Nordin

Received: 30 October 2024
Revised: 11 January 2025
Accepted: 20 January 2025
Published: 23 January 2025

Citation: Si, Z.; Jiang, Z.; Zhang, K.; Liu, Q.; Zhu, J.; She, X.; Chen, P. Energy-Efficient Joint User Association, Backhaul Bandwidth Allocation, and Power Allocation in Cell-Free mmWave UAV Networks. *Drones* **2025**, *9*, 88. https://doi.org/10.3390/drones9020088

1. Introduction

Unmanned aerial vehicles (UAVs), acting as airborne base stations (BSs), provide communication services to ground user equipment (UE) [1–3]. Their high mobility, on-demand deployment, and ability to establish direct line-of-sight (LoS) links with UEs make them a focus of interest in existing networks and future sixth-generation (6G) systems [4]. During large-scale events, such as sporting competitions, communication congestion often occurs. Additionally, natural disasters, such as earthquakes, can severely damage traditional terrestrial communication networks, resulting in service interruptions. These disruptions significantly hinder the efficiency of post-disaster rescue and emergency response efforts. In such situations, UAV BSs (UBSs) can be rapidly deployed to address communication congestion, cover affected areas, and ensure stable communication services [5,6].

To better meet the quality-of-service (QoS) requirements of ground UEs, millimeter-wave (mmWave) frequency bands are widely used to enhance communication rates [7,8]. However, densely deployed mmWave UBSs may experience severe beam interference. To mitigate this interference, a cell-free architecture has been proposed, which can convert interference signals into useful signals, thereby improving system throughput [9]. Nevertheless, the cell-free architecture also faces several challenges, particularly unavoidable beam interference [10] and backhaul load issues. To address the backhaul load problem, we introduce an integrated access and backhaul (IAB) architecture [11,12]. In traditional cell-free architectures, the backhaul link between the central processing unit (CPU) and BSs is typically transmitted via an optical fiber. However, due to the predominance of line-of-sight (LoS) transmission paths and the impracticality of fiber optics in airborne environments, using a wireless backhaul link is more suitable. Therefore, we employ a high-altitude platform station (HAPS) [13] as the CPU, with UBSs serving as multiple APs.

HAPS has been extensively studied in wireless networks and is typically deployed at an altitude of 20 km in the stratosphere, covering a radius of 50–500 km [14]. It can directly serve ground UEs through access links or act as a super macro base station, providing stable LoS paths for access points via backhaul links [15]. In a cell-free architecture, the CPU and small base stations are connected via wireless backhaul links. In disaster-stricken or densely populated areas, meeting QoS requirements becomes critical, leading to a surge in backhaul capacity demands. Although mmWave frequencies can be used to enhance backhaul capacity, their limitations remain. Additionally, to extend the operational time of UAVs in rescue missions, power consumption must be reduced while maintaining QoS for UEs, improving energy efficiency [16].

Our proposed architecture integrates UAVs, HAPS, and mmWave bands to address these challenges and offers distinct advantages over competing technologies. First, UAVs deployed as UBSs can rapidly establish direct LoS links with ground UEs, ensuring communication services in disaster-affected areas where terrestrial networks are damaged. Second, the use of mmWave frequencies enhances communication rates, providing high-quality services for ground UEs. Third, introducing HAPS as the CPU and employing wireless backhaul links eliminates the limitations of fiber optics in airborne environments. This ensures stable LoS paths for UBSs. Finally, the proposed energy-efficient scheme for user association, backhaul bandwidth allocation, and power allocation improves energy efficiency and reduces inter-beam interference, significantly enhancing network performance. In the mmWave UAV network scenario with a user-centric cell-free network architecture, the problem is initially modeled as an optimization problem aimed at maximizing energy efficiency while meeting UE QoS rate requirements. Due to its non-convex nature, the optimization problem is decomposed into three independent subproblems. Corresponding algorithms are developed to address each subproblem separately. These subproblems are then solved through alternating optimization until convergence is achieved. The proposed scheme effectively mitigates mmWave inter-beam interference, satisfies UE QoS rate requirements, and improves energy efficiency. The main contributions are summarized as follows:

- A joint user association, backhaul bandwidth allocation, and power allocation framework for maximizing energy efficiency based on a cell-free architecture is proposed in mmWave UAV networks. The problem of maximizing energy efficiency is formulated as a joint optimization problem, while considering UE QoS rate requirements. This involves optimizing user association, backhaul bandwidth allocation, and power allocation. The approach improves UE QoS by clustering multiple mmWave UBSs, optimizing the backhaul bandwidth allocation factor to allocate bandwidth between the access and backhaul links, and refining power allocation to efficiently serve UEs.

- The joint optimization problem is a non-convex mixed-integer nonlinear fractional programming problem. The problem is decoupled into three independent subproblems: user association, backhaul bandwidth allocation, and power allocation. These subproblems are solved through alternating optimization iterations. The proposed algorithm is characterized by low computational complexity and is scalable to large-scale ultra-dense mmWave UAV networks.
- A three-stage iterative optimization algorithm is proposed. The first stage employs successive convex approximation (SCA) to establish a lower bound for the concave function and a upper bound for the convex function, facilitating Dinkelbach transformation and power convex approximation optimization. In the second stage, to determine the optimal mmWave UBS clustering scheme, we introduce a user association strategy based on energy efficiency maximization. The problem is transformed into a convex form by relaxing the integer variables into continuous ones, allowing an approximate solution using the Lagrangian method. In the third stage, we derive a closed-form expression for the optimal bandwidth allocation factor.
- The system was simulated with various network parameters to verify the proposed algorithm's effectiveness and its ability to converge quickly to a stable solution. This study also examined the effects of mmWave UBS density, cooperative UBS cluster size, and UE QoS rate requirements on network performance. The results indicate that the proposed algorithm achieves performance close to that of the global search algorithm in terms of improving system energy efficiency and meeting UE QoS rate requirements. Additionally, it significantly outperforms many other algorithms while maintaining much lower complexity.

The remainder of this paper is structured as follows: Section 2 reviews the related works. Section 3 presents the cell-free mmWave UAV system model and formulates the optimization problem. Section 4 details the proposed optimization scheme for joint user association, bandwidth allocation, and power allocation, along with its implementation. Section 5 provides numerical results and discussion. Finally, Section 6 concludes the paper.

2. Related Works

In user-centric cell-free networks, user association schemes can assist UEs in selecting better coordinated BS clusters to provide enhanced communication services [17–19]. However, these studies either do not consider mmWave frequencies [20,21] or assume that all backhaul links between UAVs and the CPU are ideal, neglecting the limitations of backhaul capacity. References [22,23] proposed a cell-free architecture for UBSs to address the severe inter-cell interference between ground UEs and adjacent UBSs. They utilized the sub-terahertz frequency band to mitigate backhaul link constraints. However, they do not consider ensuring UE QoS.

Furthermore, resource allocation plays a critical role in cell-free wireless networks [24,25]. Due to the scarcity of spectrum resources and power limitations, the allocation of bandwidth and power for both access and backhaul links directly impacts UE QoS satisfaction and system energy efficiency [26–28]. Energy efficiency is a critical performance metric in communication systems, where it plays a pivotal role in optimizing network throughput and reducing power consumption [29,30]. However, these studies do not take into account the cell-free network architecture. Reference [31] proposed a QoS configuration system architecture based on mmWave user-centric cell-free massive multiple-input multiple-output (m-MIMO) and finite blocklength coding, hybrid automatic repeat request with incremental redundancy (FBC-HARQ-IR) for 6G wireless networks, focusing on statistical latency and error rate bounds. UE QoS satisfaction is also a performance metric that cannot be overlooked in resource allocation for cell-free networks [32,33].

The joint power and user grouping problem under QoS constraints was formulated, aiming at minimizing the total transmit power. A generalized benders decomposition-based algorithm was proposed, where the primal problem and master problem are solved iteratively to approach the optimal solution [34]. Nonetheless, they fail to consider the bandwidth resource allocation between the backhaul and access links.

Thus, these studies either fail to reduce system energy consumption while ensuring UE QoS or do not utilize cell-free architectures to mitigate inter-beam interference in mmWave networks. Research addressing UE QoS and energy consumption issues under backhaul link constraints in cell-free mmWave networks is relatively scarce. Most existing studies operate under the assumption of sufficient system bandwidth and guaranteed UE QoS. However, it becomes challenging to meet the QoS requirements of all UEs in scenarios where bandwidth is limited and the number of UEs is large. Therefore, we propose a joint scheme in this user-centric mmWave UAV network for user association, backhaul bandwidth allocation, and power distribution based on energy efficiency maximization to ensure that as many UEs as possible meet their QoS requirements.

3. System Model and Problem Formulation

3.1. System Model

The system model is shown in Figure 1; we consider a downlink cell-free mmWave UAV network scenario, which comprises one HAPS and N mmWave UBSs. The HAPS is used as a CPU, which is indexed by 0. We conceptualize the HAPS as a super macro base station (SMBS). This is referred to as HAPS-SMBS. It is equipped with massive multiple-input multiple-output (m-MIMO) technology and is designed to provide connectivity across a wide range of applications [35]. The sets of N mmWave UBSs and K UEs are denoted by $\mathcal{N} = \{1, .., N\}$ and $\mathcal{K} = \{1, .., K\}$, respectively. In cell-free mmWave networks, UBSs are divided into multiple cell-free cooperative clusters to serve UEs. UEs can be simultaneously associated with multiple mmWave UBSs for data transmission. There is an overlap between the cell-free cooperative UBS clusters, meaning that a single mmWave UBS may belong to multiple clusters. The link between UBSs and the HAPS-SMBS is referred to as the backhaul link, while the link between UEs and UBSs is known as the access link [11]. It is assumed that all backhaul and access links operate in the mmWave frequency band.

3.2. mmWave Signal Propagation Model

(1) Blockage model: The HAPS system is deployed at an altitude exceeding 20 km, whereas the UBS is positioned at a relatively lower altitude of 120 m [14]. This configuration primarily results in the formation of a active line-of-sight (LoS) propagation path between the HAPS and the UBS. In contrast, communications between UBS and ground UEs can be obstructed by obstacles such as buildings and trees. mmWave signals are highly susceptible to the impact of physical blockages.

The path loss characteristics between LoS and non-line-of-sight (NLoS) paths are significantly different [9,36]. The probability of each LoS path can be expressed as $P_{LoS}(d) = \exp(-d/\rho)$, where d is the three-dimensional distance between the transmitter and the receiver, and ρ is a LoS range constant. The antenna gain is calculated using the sector antenna model [37], which assumes a constant antenna gain for all angles in both the main and side lobes.

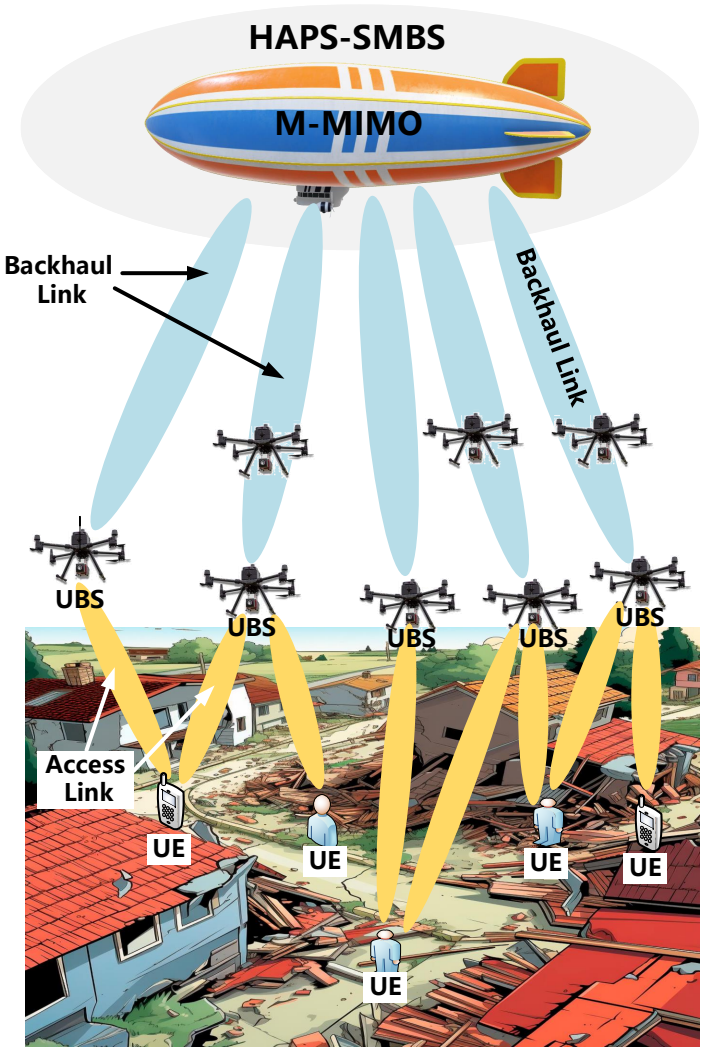

Figure 1. An IAB architecture for a cell-free mmWave UAV network for post-disaster rescue operations.

(2) mmWave beam model: Beamforming-based directional communication [37] is employed to calculate beam gain, where the beam gain in a sidelobe is a small constant $0 < \varepsilon \ll 1$. The antenna symbols are defined as shown in Table 1. Therefore, the directional beam transmission gain from mmWave UBS n to UE k can be expressed as

$$g_{nk}^{t}(\theta_n^t, \varphi_{nk}^t, \zeta_{nk}^t) = \begin{cases} \varepsilon, \text{ if } \frac{\theta_n^t}{2} < \left|\varphi_{nk}^t - \zeta_{nk}^t\right| < 2\pi - \frac{\theta_n^t}{2}, \\ \frac{2\pi - (2\pi - \theta_n^t)\varepsilon}{\theta_n^t}, \text{ otherwise.} \end{cases} \tag{1}$$

The directional beam reception gain of UE k from mmWave UBS n can be written as

$$g_{kn}^{r}(\theta_k^r, \varphi_{kn}^r, \zeta_{kn}^r) = \begin{cases} \varepsilon, \text{ if } \frac{\theta_k^r}{2} < \left|\varphi_{kn}^r - \zeta_{kn}^r\right| < 2\pi - \frac{\theta_k^r}{2}, \\ \frac{2\pi - (2\pi - \theta_k^r)\varepsilon}{\theta_k^r}, \text{ otherwise.} \end{cases} \tag{2}$$

Therefore, the effective beam gain from mmWave UBS n to UE k is defined as $G_{n,k}$, and is given by $G_{n,k} = g_{nk}^t g_{kn}^r, \forall k \in \mathcal{K}, n \in \mathcal{N}$. Similarly, the effective beam gain from mmWave HAPS-SMBS 0 to mmWave UBS n, denoted as $G_{0,n}$, can also be derived using this method.

Table 1. The definition of antenna symbols.

Symbol	Definition
θ_n^t	The beamwidth of mmWave UBS n.
θ_k^r	The beamwidth of UE k.
φ_{nk}^t	The LoS angle for mmWave UBS n to UE k.
φ_{kn}^r	The LoS angle for UE k to mmWave UBS n.
ζ_{nk}^t	The geographic position angle from mmWave UBS n to UE k.
ζ_{nk}^r	The geographic position angle for UE k to mmWave UBS n.

3.3. System Throughput Model

Let matrix $\mathbf{X}$ denote the user association indicator matrix, where the elements $x_{k,n} \in \{0,1\}$, $\forall k \in \mathcal{K}$, and $n \in \mathcal{N}$, which can be given by

$$x_{k,n} = \begin{cases} 1, & \text{if UE } k \text{ associated UBS } n, \\ 0, & \text{if UE } k \text{ not associated UBS } n. \end{cases} \tag{3}$$

Let $\mathcal{C}_k (\mathcal{C}_k \subseteq \mathcal{N})$ denote the mmWave cooperative UBS cluster of UE k, which consists of mmWave UBSs satisfying $x_{k,n} = 1$.

Define matrix $\mathbf{P}$ as the power allocation matrix, where the elements $p_{n,k}$, $\forall k \in \mathcal{K}, n \in \mathcal{N}$. $p_{n,k}$ is the power allocated to UE k by mmWave UBS n. mmWave direct beams can improve the link quality, but also introduce significant interference.

Therefore, the downlink signal-to-interference-plus-noise ratio (SINR) of UE k from the mmWave cooperative UBS cluster $\mathcal{C}_k$ can be expressed as

$$\Gamma_k = \frac{\left| \sum\limits_{n \in C_k} \sqrt{p_{n,k}} G_{n,k} h_{n,k} \right|^2}{I_k^{co} + \sigma^2} \tag{4}$$

where I_k^{co} denotes the inter-UBS cluster interference of UE k [38], σ^2 denotes additive white Gaussian noise (AWGN) of an access link, and $h_{n,k}$ denotes the channel gain between mmWave UBS n and UE k, which incorporates large-scale fading, small-scale fading, and the probability of LoS and NLoS conditions.

$$I_k^{co} = \sum_{k' \in \mathcal{K} \setminus k} \left| \sum_{n' \in \mathcal{N} \setminus \mathcal{C}_k} \sqrt{p_{n',k'}} G_{n',k} h_{n',k} \right|^2 \tag{5}$$

The downlink SINR of UE k from mmWave UBS n can be written as

$$\Gamma_{n,k} = \frac{p_{n,k} G_{n,k} h_{n,k}}{I_{n,k}^{nco} + \sigma^2} \tag{6}$$

The inter-UBS interference of UE k is denoted by

$$I_{n,k}^{nco} = \sum_{k' \in \mathcal{K} \setminus k} \left| \sum_{n' \in \mathcal{N} \setminus n} \sqrt{p_{n',k'}} G_{n',k} h_{n',k} \right|^2 \tag{7}$$

To fully exploit the directionality of mmWave communications, it is assumed that the entire access link bandwidth is multiplexed among all mmWave UBSs and UEs. Let B represent the total available bandwidth, and let β denote the backhaul bandwidth allocation

factor, which indicates the proportion of the total bandwidth allocated to a backhaul link, where $0 \leqslant \beta \leqslant 1$ [39]. Consequently, according to Shannon's formula, the access link rate for UE k from the mmWave UBS cluster $\mathcal{C}_k$ and the access link rate for UE k from mmWave UBS n are respectively expressed as follows:

$$R_k = (1-\beta)B\log_2(1+\Gamma_k) \tag{8}$$

$$R_{n,k} = (1-\beta)B\log_2(1+\Gamma_{n,k}) \tag{9}$$

The sum rate of the cell-free access link is

$$R_{sum} = \sum_{k\in\mathcal{K}} R_k \tag{10}$$

The backhaul link rate from HAPS-SMBS 0 to UBS n is given by

$$R_{0,n} = \beta B\log_2\left(1+\frac{p_{0,n}G_{0,n}h_{0,n}}{\sigma_1^2}\right) \tag{11}$$

where $h_{0,n}$ denotes the channel gain between HAPS-SMBS 0 and UBS n, and $p_{0,n}$ represents the transmission power allocated to UBS n by HAPS-SMBS 0. σ_1^2 is the AWGN power of a backhaul link. For simplicity, we assume $\sigma_1^2 = \sigma^2$ [40,41].

3.4. System Energy Modeling

To accurately characterize the energy consumption in a cell-free mmWave network, both the power consumed by the access link and the backhaul link are considered. In both links, energy consumption is divided into two components: transmission power consumption and circuit intrinsic power consumption. The former refers to the dynamic total transmitted power, while the latter corresponds to the static inherent circuit power. The total energy consumption of the backhaul link in the mmWave network can be expressed as

$$P_{sum}^{M} = \sum_{n\in\mathcal{N}} (\phi p_{0,n} + \omega_{0,n}) \tag{12}$$

where ϕ represents the reciprocal of HAPS-SMBS power amplifier efficiency. $\omega_{0,n}$ denotes the unit circuit fixed power consumption of the backhaul link between HAPS-SMBS 0 and UBS n, including the power consumption of components such as transmission filter, mixer, frequency synthesizer, and digital-to-analog converter.

The total energy consumption of the access link in a cell-free mmWave network can be expressed as

$$P_{sum}^{S} = \sum_{n\in\mathcal{N}}\sum_{k\in\mathcal{K}} x_{k,n}(\xi_n p_{n,k} + \vartheta_{n,k}) \tag{13}$$

where ξ_n represents the reciprocal of the power amplifier efficiency of mmWave UBS n, and $\vartheta_{n,k}$ denotes the unit circuit fixed power consumption of the access link between mmWave UBS n and UE k.

Therefore, the total system power consumption is the sum of the power consumption of a backhaul link and an access link, which can be expressed as

$$P_{sum} = P_{sum}^{M} + P_{sum}^{S} \tag{14}$$

3.5. Problem Formulation

The joint optimization of energy-efficient cell-free user association, backhaul bandwidth allocation, and power allocation in networks is investigated, with energy efficiency as the performance criterion. The objective is to achieve an optimal balance between system

throughput and the increase in power consumption. Energy efficiency is defined as the ratio of system throughput to power consumption and is expressed as

$$\eta_{EE} = \frac{R_{sum}}{P_{sum}} \tag{15}$$

NOTE 1: Here, we define energy efficiency as the ratio of system throughput to total energy consumption [40,41]. However, another promising performance metric is the sum of individual ratios of UE's rate to UE's energy consumption. This metric holds significant potential and will be explored further in our future research endeavors [42].

The objective of the joint cell-free user association and power allocation optimization problem is to maximize energy efficiency while satisfying the UE QoS rate requirements. Therefore, this optimization problem can be formulated as

$$\mathbb{P}0: \max_{\mathbf{X},\beta,\mathbf{P}} \eta_{EE} = \frac{R_{sum}}{P_{sum}} \tag{16a}$$

$$s.t.\ 0 \leq \sum_{k\in\mathcal{K}} x_{k,n} \leq K_{\max}, \forall n \in \mathcal{N} \tag{16b}$$

$$0 \leq \sum_{n\in\mathcal{N}} x_{k,n} \leq N_{\max}, \forall k \in \mathcal{K} \tag{16c}$$

$$p_{n,k} \geq 0, \sum_{k\in\mathcal{K}} p_{n,k} \leq p_n^{\max}, \forall k \in \mathcal{K}, n \in \mathcal{N} \tag{16d}$$

$$R_k \geq R_{k,\min}, \forall k \in \mathcal{K} \tag{16e}$$

$$\sum_{k\in\mathcal{K}} R_{n,k} \leqslant R_{0,n}, \forall n \in \mathcal{N} \tag{16f}$$

$$0 \leqslant \beta \leqslant 1 \tag{16g}$$

$$x_{k,n} \in \{0,1\}, \forall k \in \mathcal{K}, n \in \mathcal{N} \tag{16h}$$

where (16b) and (16c) are the quotas for mmWave UBSs and UEs, respectively, ensuring that each mmWave UBS n serves at most K_{max} UEs simultaneously and each UE k associates with a maximum of N_{max} mmWave UBSs concurrently. The power constraint for each mmWave UBS is given by (16d). (16e) guarantees the QoS rate requirement for each UE. (16f) guarantees that the backhaul occupancy of each mmWave UBS cannot exceed its backhaul capacity constraint. Finally, (16g) indicates the range of values for the backhaul bandwidth allocation factor.

3.6. Dinkelbach Transformation

The Dinkelbach transformation method is a potent tool for addressing fractional programming problems, with its application predicated on the conditions that the numerator of the objective function is concave, the denominator is convex, and all constraint conditions must be convex [42–44].

Theorem 1. *The optimization problem $\mathbb{P}^*0$ achieves the maximum value $\eta^* = \max_{\mathbf{Y}} \frac{F(\mathbf{Y})}{G(\mathbf{Y})}$ if and only if the following conditions are satisfied [42–44]:*

$$\max_{\mathbf{Y}} F(\mathbf{Y}) - \eta^* G(\mathbf{Y}) = F(\mathbf{Y}^*) - \eta^* G(\mathbf{Y}^*) = 0 \tag{17}$$

where $F(\mathbf{Y})$ is a concave function, $G(\mathbf{Y})$ is a convex function, and $\mathbf{Y}$ is the convex set. $\mathbf{Y}^*$ denotes the optimal values of the variables at this maximum value of the optimization problem $\mathbb{P}^*0$.

The optimization problem $\mathbb{P}0$ is inherently a non-convex mixed-integer nonlinear optimization problem, characterized by the presence of 0–1 integer variables $x_{k,n}$ and the

non-convex function R_k dependent on the continuous variable $p_{k,n}$. These features render the problem difficult to solve directly. To address this challenge, the optimization problem is decoupled into three subproblems: user association, backhaul bandwidth allocation, and power allocation. Each subproblem is tackled independently through an iterative approach, with the overall solution obtained by alternating iterations. At the end of each iteration, $\mathbb{P}0$ can be transformed into a convex optimization problem. The system model is shown in Figure 2. The detailed procedure is presented in the following sections.

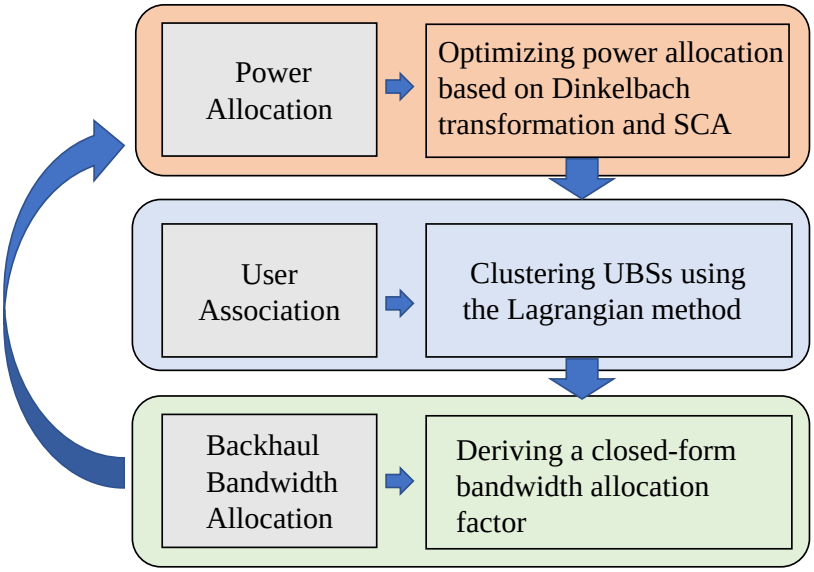

Figure 2. Flowchart of the proposed algorithm.

4. Proposed Joint Scheme for User Association, Backhaul Bandwidth Allocation Factor, and Power Allocation

To solve the joint optimization problem $\mathbb{P}0$, an iterative scheme is proposed that focuses on user association, backhaul bandwidth allocation, and power allocation. The problem $\mathbb{P}0$ is decomposed into three distinct subproblems: power allocation subproblem subproblem $\mathbb{P}1.1$, user association subproblem $\mathbb{P}1.2$, and backhaul bandwidth allocation factor subproblem $\mathbb{P}1.3$, each of which is solved independently. Specifically, the cell-free mmWave network energy efficiency is iteratively updated based on the obtained user-centered overlapping clusters until convergence is achieved.

Given the user association $\mathbf{X}$ and the backhaul bandwidth allocation factor β, the optimization problem $\mathbb{P}0$ is transformed into a power allocation problem $\mathbb{P}1.1$, as follows:

$$\mathbb{P}1.1: \quad \max_{\mathbf{P}} \eta_{EE} = \frac{R_{sum}}{P_{sum}} \tag{18a}$$

$$s.t. \quad p_{n,k} \geq 0, \sum_{k \in \mathcal{K}} p_{n,k} \leq p_n^{\max}, \forall k \in \mathcal{K}, n \in \mathcal{N} \tag{18b}$$

$$R_k \geq R_{k,\min}, \forall k \in \mathcal{K} \tag{18c}$$

$$\sum_{k \in \mathcal{K}} R_{n,k} \leqslant R_{0,n}, \forall n \in \mathcal{N} \tag{18d}$$

Given a fixed power allocation $\mathbf{P}$ and a backhaul bandwidth allocation factor β, the optimization problem $\mathbb{P}0$ is transformed into a user association problem $\mathbb{P}1.2$, as follows:

$$\mathbb{P}1.2: \max_{\mathbf{X}} \eta_{EE} = \frac{R_{sum}}{P_{sum}} \tag{19a}$$

$$s.t.\ 0 \leq \sum_{k\in\mathcal{K}} x_{k,n} \leq K_{\max}, \forall n \in \mathcal{N} \tag{19b}$$

$$0 \leq \sum_{n\in\mathcal{N}} x_{k,n} \leq N_{\max}, \forall k \in \mathcal{K} \tag{19c}$$

$$R_k \geq R_{k,\min}, \forall k \in \mathcal{K} \tag{19d}$$

$$\sum_{k\in\mathcal{K}} R_{n,k} \leqslant R_{0,n}, \forall n \in \mathcal{N} \tag{19e}$$

$$x_{k,n} \in \{0,1\}, \forall k \in \mathcal{K}, n \in \mathcal{N} \tag{19f}$$

Given the user association **X** and the fixed power allocation **P**, the optimization problem $\mathbb{P}0$ is transformed into a backhaul bandwidth allocation problem $\mathbb{P}1.3$, as follows:

$$\mathbb{P}1.3: \max_{\beta} \eta_{EE} = \frac{R_{sum}}{P_{sum}} \tag{20a}$$

$$s.t.\ R_k \geq R_{k,\min}, \forall k \in \mathcal{K} \tag{20b}$$

$$\sum_{k\in\mathcal{K}} R_{n,k} \leqslant R_{0,n}, \forall n \in \mathcal{N} \tag{20c}$$

$$0 \leqslant \beta \leqslant 1 \tag{20d}$$

4.1. Power Allocation Based on Successive Convex Approximation

Given the user association matrix **X** and the backhaul bandwidth allocation factor β, the original optimization problem $\mathbb{P}0$ is transformed into a power allocation subproblem $\mathbb{P}1.1$. The convexity of the power constraint (18b) is straightforward to verify. Since the objective function (18a), constraints (18c), and (18d) are non-convex, the optimization problem $\mathbb{P}1.1$ is still non-convex. To solve the non-convex problem $\mathbb{P}1.1$, the Dinkelbach transformation method and successive convex approximation (SCA) method are used to transform it into a series of convex subproblems. Specifically, the access link rate from the mmWave UBS cluster $\mathcal{C}_k$ to UE k, as well as from the mmWave UBS n to UE k, is relaxed and reformulated into convex functions. The access link rate from the mmWave UBS cluster $\mathcal{C}_k$ to UE k can be rewritten as

$$R_k = f_k(\mathbf{P}) - g_k(\mathbf{P}) \tag{21}$$

The access link rate from mmWave UBS n to UE k can be rewritten as

$$R_{n,k} = f_{n,k}(\mathbf{P}) - g_{n,k}(\mathbf{P}) \tag{22}$$

where

$$f_k(\mathbf{P}) = (1-\beta)B\log_2\left(\left|\sum_{n\in C_k}\sqrt{p_{n,k}}G_{n,k}h_{n,k}\right|^2 + I_k^{co} + \sigma^2\right) \tag{23}$$

$$g_k(\mathbf{P}) = (1-\beta)B\log_2\left(I_{n,k}^{co} + \sigma^2\right) \tag{24}$$

$$f_{n,k}(\mathbf{P}) = (1-\beta)B\log_2\left(p_{n,k}G_{n,k}h_{n,k} + I_{n,k}^{nco} + \sigma^2\right) \tag{25}$$

$$g_{n,k}(\mathbf{P}) = (1-\beta)B\log_2\left(I_{n,k}^{nco} + \sigma^2\right) \tag{26}$$

It can be readily demonstrated that $f_k(\mathbf{P})$, $g_k(\mathbf{P})$, $f_{n,k}(\mathbf{P})$, and $g_{n,k}(\mathbf{P})$ are concave functions. Consequently, both $R_k(\mathbf{P})$ and $R_{n,k}(\mathbf{P})$ are the difference of concave functions. The optimization problem $\mathbb{P}1.1$ represents a typical differential convex programming

problem. Utilizing the first-order Taylor approximation, the following relaxed upper bounds for $g_k(\mathbf{P})$ and $f_{n,k}(\mathbf{P})$ can be derived:

$$g_k(\mathbf{P}) \leqslant g_k\left(\mathbf{P}^l\right) + \nabla g_k\left(\mathbf{P}^l\right)^{\mathrm{T}}\left(\mathbf{P} - \mathbf{P}^l\right) \tag{27}$$

$$f_{n,k}(\mathbf{P}) \leqslant f_{n,k}\left(\mathbf{P}^l\right) + \nabla f_{n,k}\left(\mathbf{P}^l\right)^{\mathrm{T}}\left(\mathbf{P} - \mathbf{P}^l\right) \tag{28}$$

where ∇ denotes the gradient operation. Each element of $\nabla g_k\left(\mathbf{P}^l\right)$ and $\nabla f_{n,k}\left(\mathbf{P}^l\right)$ can be divided into

$$\frac{\partial\left(g_k\left(\mathbf{P}^l\right)\right)}{\partial p_{n,k}} = \begin{cases} \frac{(1-\beta)B}{\ln 2\left(I_k^{co}+\sigma^2\right)}\frac{\partial I_k^{co}}{\partial p_{n,k}} & \text{if } k = k', \\ 0, & \text{if } k \neq k'. \end{cases} \tag{29}$$

$$\frac{\partial\left(f_{n,k}\left(\mathbf{P}^l\right)\right)}{\partial p_{n,k}} = \begin{cases} \frac{(1-\beta)B}{\ln 2\left(p_{n,k}G_{n,k}h_{n,k}+I_{n,k}^{nco}+\sigma^2\right)}, & \text{if } k = k', \\ \frac{(1-\beta)BG_{n,k}h_{n,k}}{\ln 2\left(p_{n,k}G_{n,k}h_{n,k}+I_{n,k}^{nco}+\sigma^2\right)}\frac{\partial I_{n,k}^{nco}}{\partial p_{n,k}}, & \text{if } k \neq k'. \end{cases} \tag{30}$$

Let $L_k(\mathbf{P})$ denote the lower bound of the UE rate R_k, and $U_{n,k}(\mathbf{P})$ denote the upper bound of the UE rate $R_{n,k}$, respectively; then,

$$L_k(\mathbf{P}) = f_k(\mathbf{P}) - g_n\left(\mathbf{P}^l\right) - \nabla g_n\left(\mathbf{P}^l\right)^{\mathrm{T}}\left(\mathbf{P} - \mathbf{P}^l\right) \tag{31}$$

$$U_{n,k}(\mathbf{P}) = f_{n,k}\left(\mathbf{P}^l\right) + \nabla f_{n,k}\left(\mathbf{P}^l\right)^{\mathrm{T}}\left(\mathbf{P} - \mathbf{P}^l\right) - g_{n,k}(\mathbf{P}) \tag{32}$$

The upper and lower bounds are attained if and only if $\mathbf{P} = \mathbf{P}^l$. Incorporating $L_k(\mathbf{P})$ and $U_{n,k}(\mathbf{P})$ into the optimization problem $\mathbb{P}1.1$, the problem $\mathbb{P}1.1$ can be reformulated as

$$\mathbb{P}2.1: \max_{\mathbf{P}} \eta_{EE} = \frac{\sum_{k\in\mathcal{K}} L_k(\mathbf{P})}{P_{sum}(\mathbf{P})} \tag{33a}$$

$$s.t.\ \ p_{n,k} \geq 0, \sum_{k\in\mathcal{K}} p_{n,k} \leq p_n^{\max}, \forall n \in \mathcal{N}, k \in \mathcal{K} \tag{33b}$$

$$L_k(\mathbf{P}) \geq R_{k,\min}, \forall k \in \mathcal{K} \tag{33c}$$

$$\sum_{k\in\mathcal{K}} U_{n,k}(\mathbf{P}) \leq R_{0,n}, \forall n \in \mathcal{N} \tag{33d}$$

It is evident that the optimization problem $\mathbb{P}2.1$ falls into the category of typical fractional programming, characterized by a concave numerator, which stems from the concavity of the function $L_k(\mathbf{P})$, retaining its concavity when summed, whereas the denominator is convex. Additionally, $U_{n,k}(\mathbf{P})$ is convex with respect to the continuous variable $\mathbf{P}$, thereby ensuring that the feasible solution set defined by the constraints (33b), (33c), and (33d) is convex. Consequently, according to Theorem 1, the Dinkelbach transformation method can be employed to convert it into a more tractable form.

$$\mathbb{P}2.2: \max_{\mathbf{P}} \sum_{k\in\mathcal{K}} L_k(\mathbf{P}) - \eta_{EE} P_{sum}(\mathbf{P}) \tag{34a}$$

$$s.t.\ \ p_{n,k} \geq 0, \sum_{k\in\mathcal{K}} p_{n,k} \leq p_n^{\max}, \forall n \in \mathcal{N}, k \in \mathcal{K} \tag{34b}$$

$$L_k(\mathbf{P}) \geq R_{k,\min}, \forall k \in \mathcal{K} \tag{34c}$$

$$\sum_{k\in\mathcal{K}} U_{n,k}(\mathbf{P}) \leq R_{0,n}, \forall n \in \mathcal{N} \tag{34d}$$

It is evident that the optimization problem $\mathbb{P}2.2$ is a convex optimization problem. The reason is that the objective function (34a) is concave with respect to the continuous variable $\mathbf{P}$. Additionally, the feasible solution set defined by the constraints (34b), (34c), and (34d) is convex. The optimization problem $\mathbb{P}2.2$ can be efficiently solved using the interior point method [45,46], and the detailed procedure is outlined in Algorithm 1.

Algorithm 1 Power Allocation Algorithm Based on Dinkelbach Transformation and SCA Method

1: **Initialization:** Minimum convergence threshold δ, maximum number of iterations τ_{max}, number of iterations $l = 0$.
2: Dinkelbach transformation method
3: **repeat**
4: Given η_{EE}, solve the optimization problem $\mathbb{P}2.2$ using the interior point method to obtain $\mathbf{P}^*$;
5: Update $\mathbf{P}^{l+1} = \mathbf{P}^*$;
6: Update $l = l + 1$.
7: **until** $\left|\mathbf{P}^{l+1} - \mathbf{P}^{l}\right| < \delta$ or $l = l_{max}$.
8: **Output**: The optimal power allocation $\mathbf{P}$.

4.2. User Association Based on Energy Efficiency Maximization in Cell-Free mmWave UAV Network

Given a fixed power allocation $\mathbf{P}$ and a backhaul bandwidth allocation factor β, the optimization problem $\mathbb{P}0$ is transformed into a user association problem $\mathbb{P}1.2$. This subproblem addresses the formation of UBS clusters in a cell-free mmWave network. This goal is pursued by simultaneously increasing the UE rate and minimizing power consumption. In practice, prior to the formation of cell-free clusters, it is not feasible to precisely compute the rate that UE k obtains from a cell-free cluster. However, we can utilize the data rate from the cellular network architecture to roughly estimate the achievable data rate when UE k is associated with a single UBS. Therefore, $r_{n,k} = x_{k,n} R'_{n,k}$ is employed as an approximation for the rate of UE k, where $R'_{n,k} = (1-\beta) B \log(1 + \Gamma'_{n,k})$, $\Gamma'_{n,k} = \frac{p_{n,k} G_{n,k} h_{n,k}}{\sum_{k'\in\mathcal{K}\setminus k} \sum_{n'\in\mathcal{N}\setminus n} p_{n',k'} G_{n',k} h_{n',k} + \sigma^2}$.

From the perspective of the UEs, UEs naturally prefer mmWave UBSs that offer high data rates and low power consumption. For each UE k, the utility derived from associating with mmWave UBS n can be expressed as $r_{n,k} - x_{k,n}\eta_{EE}(\xi_n p_{n,k} + \vartheta_{n,k})$. If $x_{k,n} = 1$, then $r_{n,k} = R'_{n,k}$, denoting the rate achieved by UE k when associated with mmWave UBS n. Conversely, if $x_{k,n} = 0$, it indicates that UE k is not associated with mmWave UBS n, resulting in $r_{n,k} = R'_{n,k} = 0$. From the perspective of the mmWave UBS, the selection is biased towards UEs that offer high data rates with low energy consumption. In the process of user association, due to the difficulty in predicting the rate received by UE k from its cell-free cooperative UBS cluster, we have decided to remove the original constraint (19d) and instead utilize the decision condition outlined in Algorithm 2 to guide our decision making.

Based on this principle, the user association optimization problem can be formulated as follows:

$$\mathbb{P}2.1: \max_{\mathbf{X}} \sum_{n\in\mathcal{N}} \sum_{k\in\mathcal{K}} (r_{n,k} - x_{k,n}\eta_{EE}(\xi_n p_{n,k} + \vartheta_{n,k})) \tag{35a}$$

$$s.t.\ 0 \le \sum_{k\in\mathcal{K}} x_{k,n} \le K_{\max}, \forall n \in \mathcal{N} \tag{35b}$$

$$0 \le \sum_{n\in\mathcal{N}} x_{k,n} \le N_{\max}, \forall k \in \mathcal{K} \tag{35c}$$

$$\sum_{k\in\mathcal{K}} r_{n,k} \leqslant R_{0,n}, \forall n \in \mathcal{N} \tag{35d}$$

$$x_{k,n} \in \{0,1\}, \forall k \in \mathcal{K}, n \in \mathcal{N} \tag{35e}$$

Algorithm 2 User Association Algorithm Based on Energy Efficiency Maximization in Cell-Free mmWave UAV Network

Input: Power allocation matrix $\mathbf{P}$ and backhaul bandwidth allocation factor β.
Initialization: The Lagrange multipliers $\boldsymbol{\lambda}, \boldsymbol{\gamma}, \boldsymbol{\theta}$ are zero vectors.
for each UE $k = 1, 2, .., K$ **do**
  while $\sum_{n\in\mathcal{N}} x_{k,n} < N_{\max}$ and $r_k < R_{k,min}$ **do**
    Calculate n^* according to Equation (42);
    Update $x_{k,n}$ using n^* according to Equation (41).
    for each mmWave UBS $n = 1, 2, .., N$ **do**
      if $\sum_{k\in\mathcal{K}} x_{k,n} \geqslant K_{\max}$ **then**
        $\frac{\partial \mathcal{L}(\mathbf{X},\boldsymbol{\lambda},\boldsymbol{\gamma},\boldsymbol{\theta})}{\partial x_{k+1,n}} = 0$.
      end if
      Set $\frac{\partial \mathcal{L}(\mathbf{X},\boldsymbol{\lambda},\boldsymbol{\gamma},\boldsymbol{\theta})}{\partial x_{k,n^*}} = 0$, update $\frac{\partial \mathcal{L}(\mathbf{X},\boldsymbol{\lambda},\boldsymbol{\gamma},\boldsymbol{\theta})}{\partial x_{k,n}}$.
      repeat
        Update λ_n, γ_k, θ_n according to Equations (43)–(45).
      until Convergence.
    end for
  end while
end for
Output: The user association matrix $\mathbf{X}$.

The problem $\mathbb{P}2.1$ is a non-convex 0–1 integer programming problem. It poses significant challenges due to its non-convex nature. To address this, the problem can be approached using the relaxation method combined with the Lagrangian method. If the binary variable $x_{k,n}$ is relaxed to a continuous variable such that $0 \leqslant x_{k,n} \leqslant 1$, the optimization problem $\mathbb{P}2.1$ is transformed into

$$\mathbb{P}2.3: \max_{\mathbf{X}} \sum_{n\in\mathcal{N}} \sum_{k\in\mathcal{K}} x_{k,n}\left((1-\beta)B\log_2\left(1+\Gamma'_{n,k}\right) - \eta_{EE}(\xi_n p_{n,k} + \vartheta_{n,k})\right) \tag{36a}$$

$$s.t.\ 0 \le \sum_{k\in\mathcal{K}} x_{k,n} \le K_{\max}, \forall n \in \mathcal{N} \tag{36b}$$

$$0 \le \sum_{n\in\mathcal{N}} x_{k,n} \le N_{\max}, \forall k \in \mathcal{K} \tag{36c}$$

$$\sum_{k\in\mathcal{K}} x_{k,n}(1-\beta)B\log_2\left(1+\Gamma'_{n,k}\right) \leqslant R_{0,n} \tag{36d}$$

$$0 \leqslant x_{k,n} \leqslant 1, \forall n \in \mathcal{N}, k \in \mathcal{K} \tag{36e}$$

Given a fixed power allocation and bandwidth allocation factor, any term independent of $x_{k,n}$ is treated as a constant. The objective function of $\mathbb{P}2.3$ in (36a) is a linear function of $x_{k,n}$, while the constraints in (36b)–(36e) evidently form a convex set with respect to

$x_{k,n}$. The convexity of $\mathbb{P}2.3$ arises from the removal of the constraint (36e). Although this operation seemingly expands the constraint set, we have incorporated an additional verification step in Algorithm 2 to check whether UE satisfies the QoS requirements, which essentially re-introduces the effect of the constraint (19d). Consequently, we consider the non-convexity issue of $\mathbb{P}2.3$ to be resolved. Therefore, it can be demonstrated that the optimization problem $\mathbb{P}2.3$ is a convex optimization problem with respect to the continuous variable $x_{k,n}$. Subsequently, the derivation will show that the solution obtained after relaxing the variables remains the optimal solution to the original problem $\mathbb{P}2.2$. By employing Lagrangian pairwise decomposition, the Lagrangian function for the problem $\mathbb{P}2.3$ is formulated as

$$\begin{aligned}\mathcal{L}(\mathbf{X},\boldsymbol{\lambda},\boldsymbol{\gamma},\boldsymbol{\theta}) = &\sum_{n\in\mathcal{N}}\sum_{k\in\mathcal{K}} x_{k,n}\left((1-\beta)B\log_2\left(1+\Gamma'_{n,k}\right)-\eta_{EE}(\xi_n p_{n,k}+\vartheta_{n,k})\right)\\ &+\sum_{n\in\mathcal{N}}\lambda_n\left(K_{\max}-\sum_{k\in\mathcal{K}}x_{k,n}\right)+\sum_{k\in\mathcal{K}}\gamma_k\left(N_{\max}-\sum_{n\in\mathcal{N}}x_{k,n}\right)\\ &+\sum_{n\in\mathcal{N}}\theta_n\left(R_{0,n}-\sum_{k\in\mathcal{K}}x_{k,n}(1-\beta)B\log_2\left(1+\Gamma'_{n,k}\right)\right)\end{aligned} \tag{37}$$

where $\boldsymbol{\lambda}$, $\boldsymbol{\gamma}$, and $\boldsymbol{\theta}$ are the dual variables associated with the constraints (36b), (36c), and (36d) , respectively. The dual problem of $\mathbb{P}2.3$ can be expressed as

$$\mathbb{P}2.4: \min_{\boldsymbol{\lambda},\boldsymbol{\gamma},\boldsymbol{\theta}} d(\mathbf{X},\boldsymbol{\lambda},\boldsymbol{\gamma},\boldsymbol{\theta}) \tag{38a}$$

$$s.t. \boldsymbol{\lambda}\geq 0, \boldsymbol{\gamma}\geq 0, \boldsymbol{\theta}\geq 0 \tag{38b}$$

where

$$d(\boldsymbol{\lambda},\boldsymbol{\gamma},\boldsymbol{\theta}) = \max_{\mathbf{X}} \mathcal{L}(\mathbf{X},\boldsymbol{\lambda},\boldsymbol{\gamma},\boldsymbol{\theta}) \tag{39}$$

The first-order partial derivatives of $\mathcal{L}$ with respect to $x_{k,n}$ is

$$\begin{aligned}\frac{\partial\mathcal{L}(\mathbf{X},\boldsymbol{\lambda},\boldsymbol{\gamma},\boldsymbol{\theta})}{\partial x_{k,n}} = &(1-\beta)B\log_2\left(1+\Gamma'_{n,k}\right)-\eta_{EE}(\xi_n p_{n,k}+\vartheta_{n,k})\\ &-\lambda_n-\gamma_k-\theta_n(1-\beta)B\log_2\left(1+\Gamma'_{n,k}\right)\end{aligned} \tag{40}$$

Define the elements of the user association matrix $\mathbf{X}$ in the subproblem $\mathbb{P}2.3$ as those that satisfy the following conditions:

$$x_{k,n} = \begin{cases} 1, & \text{if } n = n^*, \\ 0, & \text{if } n \neq n^*. \end{cases} \tag{41}$$

where

$$n^* = \arg\max_{n\in\mathcal{N}} \begin{pmatrix} (1-\beta)B\log_2\left(1+\Gamma'_{n,k}\right)-\eta_{EE}(\xi_n p_{n,k}+\vartheta_{n,k}) \\ -\lambda_n-\gamma_k-\theta_n(1-\beta)B\log_2\left(1+\Gamma'_{n,k}\right) \end{pmatrix} \tag{42}$$

Equation (41) can be considered a judgment criterion for UEs to determine the optimal mmWave UBS. Additionally, the Lagrange multipliers can be updated using the subgradient method, which can be expressed as

$$\lambda_n(t+1) = \left[\lambda_n(t)-\delta_1(t)\left(K_{\max}-\sum_{k\in\mathcal{K}}x_{k,n}(t)\right)\right]^+ \tag{43}$$

$$\gamma_k(t+1) = \left[\gamma_k(t)-\delta_2(t)\left(N_{\max}-\sum_{k\in\mathcal{K}}x_{k,n}(t)\right)\right]^+ \tag{44}$$

$$\theta_n(t+1) = \left[\theta_n(t) - \delta_3(t)\left(R_{0,n} - \sum_{k\in\mathcal{K}} x_{k,n}(t)(1-\beta)B\log_2\left(1+\Gamma'_{n,k}\right)\right)\right]^+ \tag{45}$$

where $[a]^+ = \max\{0, a\}$. $\delta_1(t)$, $\delta_2(t)$ and $\delta_3(t)$ denote the step size. By updating the Lagrangian multipliers, the dual problem becomes globally optimal when the multipliers converge. Slater's condition is a suitable constraint qualification for concave maximization problems subject to convex constraints [42,45,47]. When Slater's conditions are satisfied and the primal problem is convex, a strong duality is established. It is evident, based on the problem formulation, that the feasible region is proven to be a convex set. Furthermore, the constraint function (36a) has been verified to be convex. More importantly, we can readily identify a specific solution $x_{k,n}$ that is neither zero nor one, yet strictly satisfies all the constraint conditions. Consequently, we can confidently assert that Slater's condition holds in the problem $\mathbb{P}2.3$.

The user association algorithm based on cell-free and maximum energy efficiency is summarized by Algorithm 2. As described in Algorithm 2, UEs sequentially select their associated UBSs. Each UE_k always chooses up to N_{MAX} UBSs with the highest utility function values for association. Provided that the selected UBSs can fulfill the QoS requirements of UE_k, the process then proceeds to associate the next UE with its respective UBSs.

4.3. Backhaul Link Bandwidth Allocation Factor Optimization

After completing the mmWave UBS clustering, the user association matrix $\mathbf{X} = \mathbf{X}^*$ is obtained. Subsequently, the backhaul bandwidth allocation factor β is determined. With the fixed power allocation results and the established user association matrix, the optimization problem $\mathbb{P}0$ can be simplified as $\mathbb{P}1.3$. The objective function of the optimization problem $\mathbb{P}1.3$ can be expressed as

$$\max_{\beta} \eta_{EE} = \frac{\sum_{k\in\mathcal{K}}(1-\beta)B\log_2(1+\Gamma_k)}{P_{sum}} \tag{46}$$

It is evident that the objective function of the optimization problem $\mathbb{P}1.3$ is a monotone decreasing function. Therefore, maximizing this function is equivalent to maximizing $1-\beta$. The constraints for the optimization problem $\mathbb{P}1.3$ are subsequently reformulated. From the constraint (20b), the following can be derived:

$$\beta \leqslant 1 - \frac{R_{k,\min}}{B\log_2\left(1+\frac{\left|\sum_{n\in C_k}\sqrt{p_{n,k}}G_{n,k}h_{n,k}\right|^2}{I_k^{co}+\sigma^2}\right)} \tag{47}$$

Based on the constraint (20c), it is obtained that

$$\beta \geqslant \frac{\sum_{k\in\mathcal{K}}\log_2\left(1+\frac{p_{n,k}G_{n,k}h_{n,k}}{I_{n,k}^{nco}+\sigma^2}\right)}{\log_2\left(1+\frac{p_{0,n}G_{0,n}h_{0,n}}{\sigma^2}\right)+\sum_{k\in\mathcal{K}}\log_2\left(1+\frac{p_{n,k}G_{n,k}h_{n,k}}{I_{n,k}^{nco}+\sigma^2}\right)} \tag{48}$$

Therefore, a closed-form expression for the backhaul bandwidth allocation factor β can be obtained.

$$\beta = \max_{n\in\mathcal{N}}\{\Psi_n\} \tag{49}$$

Simultaneously, it needs to satisfy

$$\beta \leqslant \Upsilon_n \tag{50}$$

where

$$\Psi_n = \frac{\sum\limits_{k\in\mathcal{K}} \log_2\left(1+\frac{p_{n,k}G_{n,k}h_{n,k}}{I_{n,k}^{nco}+\sigma^2}\right)}{\log_2\left(1+\frac{p_{0,n}G_{0,n}h_{0,n}}{\sigma^2}\right)+\sum\limits_{k\in\mathcal{K}} \log_2\left(1+\frac{p_{n,k}G_{n,k}h_{n,k}}{I_{n,k}^{nco}+\sigma^2}\right)} \tag{51}$$

$$\Upsilon_n = 1 - \frac{R_{k,\min}}{B\log_2\left(1+\frac{\left|\sum\limits_{n\in C_k}\sqrt{p_{n,k}}G_{n,k}h_{n,k}\right|^2}{I_k^{co}+\sigma^2}\right)} \tag{52}$$

The optimization process for the backhaul bandwidth allocation factor β is outlined in Algorithm 3. In this process, each mmWave UBS $n \in \mathcal{N}$ computes the values of Ψ_n and Υ_n per Equations (51) and (52). These values are subsequently communicated to the HAPS-SMBS. The HAPS-SMBS then selects the maximum Ψ_n as the optimal bandwidth allocation factor β. This selected β is broadcast to allocate bandwidth for the backhaul link between the HAPS-SMBS and each UBS. Simultaneously, the factor $1-\beta$ is broadcast to manage bandwidth allocation for the access link between each UBS and UE.

Algorithm 3 Backhaul Bandwidth Factor β Optimization

1: **for** each mmWave UBS $n = 1, 2, .., N$ **do**
2: Calculate Ψ_n and Υ_n according to Equations (51) and (52) and feed back to HAPS-SMBS.
3: **end for**
4: Find $\beta = \max\limits_{n\in\mathcal{N}}\{\Psi_n\}$ and satisfies $\beta \leqslant \Upsilon_n$ in HAPS-SMBS side;
5: Use β as the optimal backhaul bandwidth allocation factor;
6: Broadcast β to the backhaul link and $1-\beta$ to the access link.
7: **Output**: The optimal backhaul bandwidth allocation factor β and $\eta_{EE} = \frac{R_{sum}}{P_{sum}}$.

4.4. Joint User Association, Backhaul Bandwidth, and Power Allocation Alternate Optimization Based on Maximum Energy Efficiency

After providing solutions for each subproblem, the overall algorithm for solving the optimization problem $\mathbb{P}0$ is presented. Initially, the backhaul bandwidth allocation factor and power allocation are initialized, with each HAPS-SMBS uniformly allocating transmission power to each UBS on the backhaul link. During each iteration, the process involves sequential optimization of the three variables: user association, backhaul bandwidth allocation factor, and power allocation. Each variable is optimized in turn, while the other two variables are held constant, as detailed in Algorithm 4.

In the τ iteration of Algorithm 4, given $(\mathbf{X}^\tau, \beta^\tau)$, the power allocation optimization is performed, and the power optimization matrix $\mathbf{P}^{\tau+1}$ is updated by executing Algorithm 1. Next, given $\left(\beta^\tau, \mathbf{P}^{\tau+1}\right)$, the mmWave UBS clustering is performed first by executing Algorithm 2 to obtain the user association matrix $\mathbf{X}^{\tau+1}$. Finally, with $\left(\mathbf{X}^{\tau+1}, \mathbf{P}^{\tau+1}\right)$ fixed, Algorithm 3 is executed. Additionally, each mmWave UBS calculates Ψ_n and Υ_n according to Equations (51) and Equations (52), respectively. These values are then fed back to the HAPS-SMBS, which selects the maximal Ψ_n as the optimal bandwidth allocation factor $\beta^{\tau+1}$. The HAPS-SMBS broadcasts $\beta^{\tau+1}$ for use in the bandwidth allocation of the backhaul link between the HAPS-SMBS and each UBS, and broadcasts $1-\beta^{\tau+1}$ for the access link bandwidth allocation between the UBS and UE. As the number of iterations increases,

$R_{sum}^{\tau} - \eta_{EE}^{\tau} P_{sum}^{\tau}$ monotonically increases, and since an upper bound exists, the iterative process of Algorithm 4 is guaranteed to eventually converge.

Algorithm 4 Joint User Association, Backhaul Bandwidth, and Power Allocation Alternate Optimization Algorithm Based on Energy Efficiency Maximization

1: **Input:** UBS maximal number of associations N_{max}, UBS maximal number of UEs served K_{max}, UE QoS requirement value $R_{k,min}$, maximal number of iterations τ_{max}, convergence threshold ϵ.
2: **Initialization:** Transmission power $\mathbf{P}^0$, backhaul bandwidth allocation factor $\beta^0 = 0.5$, and number of iterations $\tau = 0$. The HAPS-SMBS distributes the transmission power uniformly for each UBS. Each UE k establishes associations with the top N_{max} UBSs that are nearest in distance. Calculate R_{sum}^0 and P_{sum}^0 according to Equations (10) and (14). And calculate $\eta_{EE}^0 = \frac{R_{sum}^0}{P_{sum}^0}$.
3: **while** $R_{sum}^{\tau} - \eta_{EE}^{\tau} P_{sum}^{\tau} > \epsilon$ && $\tau < \tau_{max}$ **do**
4: Given $(\mathbf{X}^{\tau}, \beta^{\tau})$, perform Algorithm 1 to update the power allocation matrix $\mathbf{P}^{\tau+1}$;
5: Given $(\beta^{\tau}, \mathbf{P}^{\tau+1})$, execute Algorithm 2 to update the user association matrix $\mathbf{X}^{\tau+1}$;
6: Given $(\mathbf{X}^{\tau+1}, \mathbf{P}^{\tau+1})$, perform Algorithm 3 to update the backhaul bandwidth allocation factor $\beta^{\tau+1}$ and $\eta_{EE}^{\tau+1} = \frac{R_{sum}^{\tau+1}}{P_{sum}^{\tau+1}}$;
7: Update $\tau = \tau + 1$.
8: **end while**
9: **Output**: The optimal user association $\mathbf{X}^*$, backhaul bandwidth allocation factor β^*, and power allocation $\mathbf{P}^*$.

4.5. Algorithm Complexity

The computational complexity of the proposed algorithm is evaluated as follows: Since the formulated problem $\mathbb{P}0$ is not convex, the only way to obtain the optimal solution is to use the exhaustive algorithm (EA). For each iteration, UE and UBS need to compute their respective utility functions and perform pairing based on these functions. On the UE side, establishing associations with all potential pairing partners requires $N_{max}N$ computations. Considering that there are a total of K UEs in the system, the computational complexity of the entire process can be denoted as $N_{max}KN$. Therefore, the computational complexity of Algorithm 2 is $\mathcal{O}(N_{max}KN)$ [41,42]. Consequently, the overall complexity of Algorithm 2 is $\mathcal{O}(T_{ua}N_{max}KN)$, where T_{ua} denotes the number of iterations within Algorithm 2. In comparison, the complexity of the EA increases exponentially with the number of UEs and mmWave UBSs, highlighting the efficiency of Algorithm 2 in significantly reducing computational complexity relative to the EA. The computational complexity in Algorithm 3 is negligible [40,41]. For power allocation optimization, Algorithm 1 employs the interior point method, resulting in a computational complexity of $\mathcal{O}(T_{pa}N^3)$ based on the result of [45,46], where T_{pa} represents the number of iterations in Algorithm 1. The total complexity of Algorithm 4 is primarily dependent on the user association and power allocation phases, which can be expressed as $\mathcal{O}(T_{oa}(T_{ua}N_{max}KN + T_{pa}N^3))$, with T_{oa} representing the number of iterations of Algorithm 4. When the numbers of UEs and UBSs increase, the complexity of the EA increases exponentially, so the complexity of the EA is much larger than the complexities of the proposed algorithms.

5. Numerical Results and Discussion

5.1. System Parameterization

The proposed algorithm is evaluated to provide simulation results for various energy-efficient schemes in cell-free mmWave-based networks. Key simulation parameters and settings are given based on [14,48–50], as shown in Table 2. A simulation is conducted for an mmWave network with HAPS-SMBS coverage over a circular area with a radius of

3000 m, where mmWave UBSs and UEs are randomly distributed within the simulation area. The mmWave UBSs follow a homogeneous Poisson point process (PPP) distribution with density λ_N, while UEs are uniformly distributed with density λ_K [51]. Based on the 3GPP channel models [50,52], the data transmission suffers from both large-scale fading and small-scale fading. The channel model in the mmWave network is assumed to adhere to Rician fading, and the path loss model is represented by $PL = 32.4 + 21\log_{10}(d) + 20\log_{10}(f_c)$, where d denotes the three-dimensional distance between the UE and the mmWave UBS, and f_c is the center frequency. Unless otherwise specified, the key simulation parameters are shown in Table 2.

Table 2. Simulation parameters.

Parameters	Value
Bandwidth, B	2 GHz
Coverage radius	500 m
Carrier frequency, f_c	28 GHz [49]
Transmit power, $p_0^{\max}$, $p_n^{\max}$	50 dBm, 35 dBm
HAPS unit circuit power consumption, $\omega_{0,n}$	54 mW
UBS unit circuit power consumption, $\vartheta_{n,k}$	20 mW
Noise spectral density, N_0	-174 dBm/Hz
Shadow fading standard deviation	10 dB
The number of antennas equipped at each UBS	16 [53]
Beamwidth of UE k, θ_k^r	10°
Beamwidth of mmWave UBS n, θ_n^t	10°
UE density, λ_K	$200/\text{km}^2$
UBS density, λ_N	$100/\text{km}^2$
Sidelobe gain, ε	0.1
LoS range constant, ρ	150 m
Maximum number of service UEs, $K_{\max}$	16
Maximum number of associated mmWave UBSs, $N_{\max}$	3
Convergence threshold, δ, ε	10^{-4}, 10^{-4}
Maximum number of iterations, l_{max}, t_{max}, τ_{max}	100, 100, 100
QoS requirement, $R_{k,\min}$	100 Mbps
mmWave UBS height	120 m [14]
HAPS height	20 km [14]

5.2. Simulation Results and Analysis

To verify the effectiveness of the proposed algorithm (Algorithm 4), its performance is compared with that of the EA, maximum SINR (MAX-SINR), optimal channel gain (OCG), minimum distance algorithm (MDA), and random matching (RM). For a fair comparison, the user association is optimized using these algorithms, while the remaining steps are consistent with the proposed algorithm. For instance, the EA enumerates all possible user association outcomes, executes Algorithm 4, and computes the energy efficiency value. The association result with the highest energy efficiency value across the exhaustive iterations is then selected as the optimal solution.

First, the convergence of the proposed algorithm is analyzed, using the EA as a benchmark. Figure 3 presents a comparison of energy efficiency between the two algorithms for mmWave UBS densities of $100/\text{km}^2$ and $200/\text{km}^2$. It is evident that the energy efficiency of the proposed algorithm gradually approaches that of the EA as the number of iterations increases, while also achieving faster convergence.

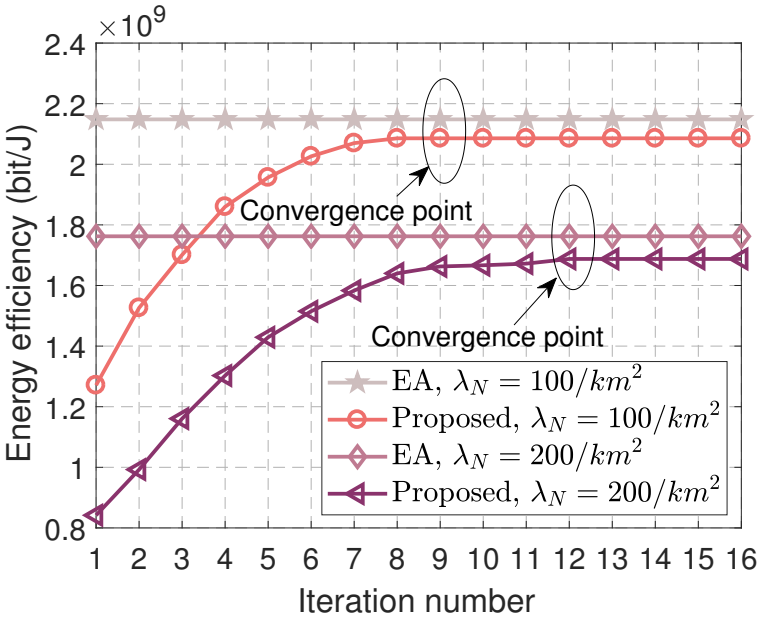

Figure 3. Convergence of Algorithm 4.

Figure 4 illustrates the impact of an mmWave UBS beamwidth on energy efficiency. As the beamwidth of the mmWave increases, the energy efficiency correspondingly decreases. This decline can be attributed to the fact that a wider beamwidth leads to greater interference and a reduction in antenna gain. Beyond a specific threshold, the transmission quality of the access link deteriorates. In such scenarios, mmWave UBSs are compelled to establish more access links to satisfy the QoS rate requirements of UEs. Figure 4 clearly demonstrates that, excluding the EA, the proposed algorithm consistently achieves the highest energy efficiency, irrespective of the beamwidth variation. Specifically, when the mmWave UBS beamwidth is $\theta_n^t = 10°$, the proposed algorithm exhibits a 16.36% gain in energy efficiency compared with the maximum SINR algorithm. This gain increases to 19.06% when $\theta_n^t = 40°$.

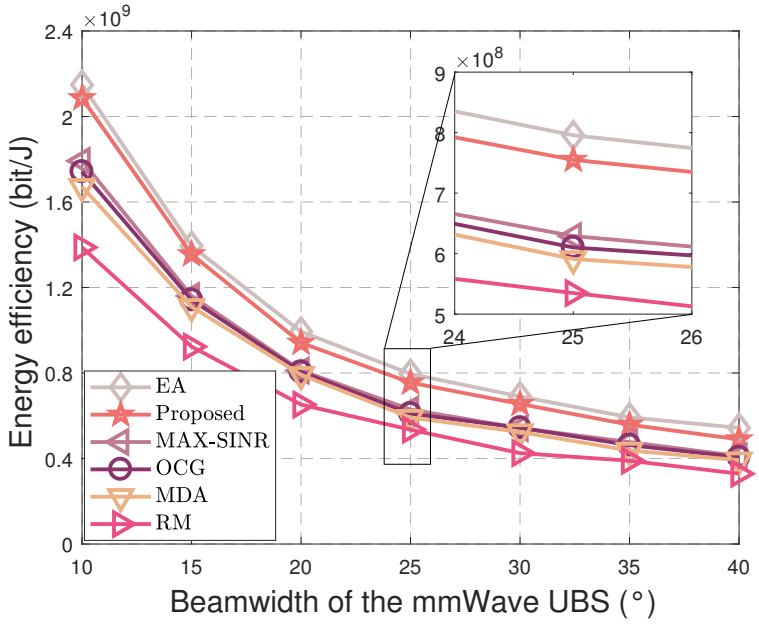

Figure 4. The energy efficiency varies with the beamwidth of the mmWave UBS.

Figure 5 depicts the impact of the cell-free cooperative UBS cluster size on energy efficiency under varying mmWave UBS and UE densities. The results indicate that as N_{max} increases, the energy efficiency of all algorithms initially rises to a peak before gradually declining. This trend can be explained by the observation that, as the number of mmWave UBSs associated with a UE increases, the cooperative gain obtained by the UE also increases, thereby enhancing both system throughput and UE transmission rates more than the system's energy consumption. Consequently, system energy efficiency improves. However, when N_{max} continues to rise, the cooperative gain starts to diminish while system energy consumption continues to grow, resulting in a reduction in overall system energy efficiency. Considering factors such as signaling overhead, system energy consumption, and UE QoS rate requirements, a default setting of $N_{max} = 3$ is deemed optimal.

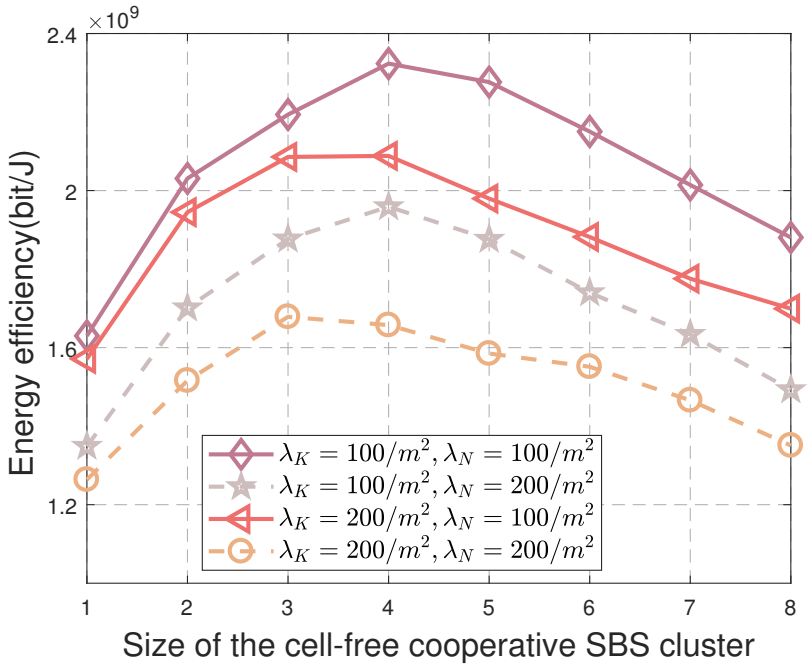

Figure 5. The energy efficiency varies with the sizes of the cell-free cooperative UBS cluster.

Figures 6 and 7 depict the variation in energy efficiency across different UBS densities and UE densities within the mmWave network. Specifically, Figure 6 presents the energy efficiency variation with respect to the mmWave UBS density when the UE density is 200/km^2. The results indicate that the energy efficiency initially increases, reaching a peak, and then gradually decreases. This trend can be attributed to the fact that, as the mmWave UBS density increases, the number of UBSs available for user association also increases, leading to continuous but diminishing growth in system throughput. When the mmWave UBS density becomes sufficiently high, intra-cluster and inter-cluster interference among the mmWave UBSs impedes further gains in throughput. At lower UBS densities, the growth in system throughput surpasses the increase in system energy consumption, resulting in improved energy efficiency. However, as the density of mmWave UBSs continues to rise, the incremental throughput gains are outpaced by the increased energy consumption, causing a gradual decline in energy efficiency. The results indicate that the proposed algorithm outperforms the maximum SINR algorithm, yielding a performance gain of 22.06% at a UE density of 50/km^2 and 8.85% at a UE density of 400/km^2.

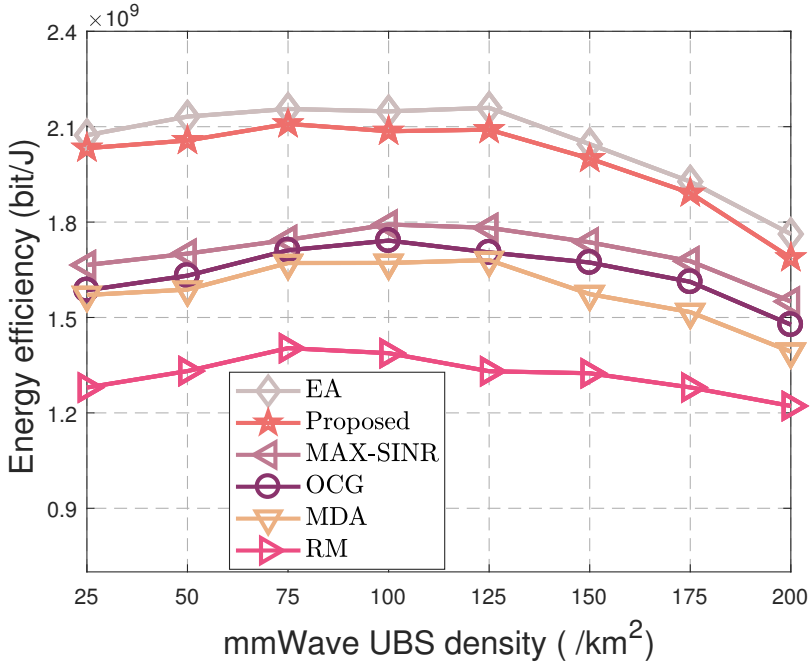

Figure 6. The energy efficiency varies with the density of the mmWave UBSs.

Figure 7 illustrates the energy efficiency variation as a function of different UE densities at a mmWave UBS density of 100/km^2. The results indicate that system energy efficiency consistently decreases as UE density increases. This can be attributed to the fact that at lower UE densities, there are ample mmWave UBSs available to serve each UE, resulting in a slower decline in energy efficiency as the number of UEs increases. However, as UE density continues to grow, more mmWave UBSs must be associated to meet the UE QoS rate requirements, leading to a significant increase in system energy consumption. Consequently, energy efficiency declines at an accelerated rate. The proposed algorithm demonstrates a performance gain of 18.01% over the maximum SINR algorithm at a UE density of 50/km^2 and 15.63% at a UE density of 400/km^2.

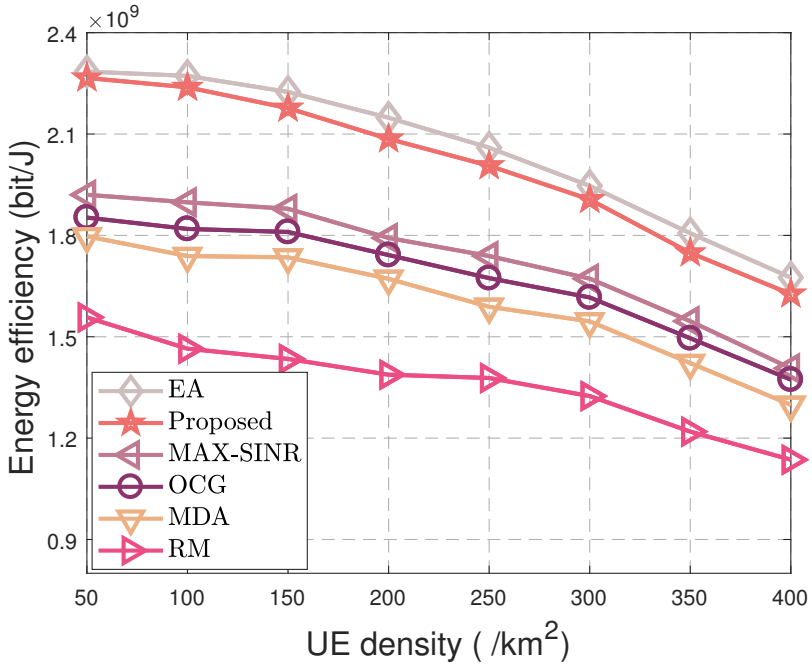

Figure 7. The energy efficiency varies with the density of the UEs.

Figure 8 examines the energy efficiency performance as a function of the maximum transmission power of the mmWave UBS. Comparisons are made against different benchmarks under the same conditions. The scenarios considered include (i) an optimal backhaul bandwidth allocation factor, where energy efficiency is maximized by optimizing relevant variables, and (ii) a fixed bandwidth allocation factor $\beta = 0.5$, where the bandwidth is equally distributed between the access link and wireless backhaul link. As shown in Figure 8, energy efficiency initially increases with transmission power for all schemes. This is because optimizing transmission power and bandwidth allocation enhances the received data rate per UE. Consequently, system throughput improves faster than transmission power consumption, leading to better energy efficiency. However, beyond a certain point, further increases in transmission power cause a decrease in energy efficiency. This decline occurs due to the trade-off between transmission data rate capability and power consumption in energy-efficient power allocation.This observation underscores that continuously increasing power is not a feasible approach to maximize energy efficiency. Moreover, Figure 8 highlights that the proposed scheme, which optimizes the backhaul bandwidth allocation factor β, achieves significantly higher energy efficiency than the fixed β scheme. At a mmWave UBS transmission power of 35 dBm, the proposed scheme shows a performance gain of 11.68% compared with the fixed β scheme.

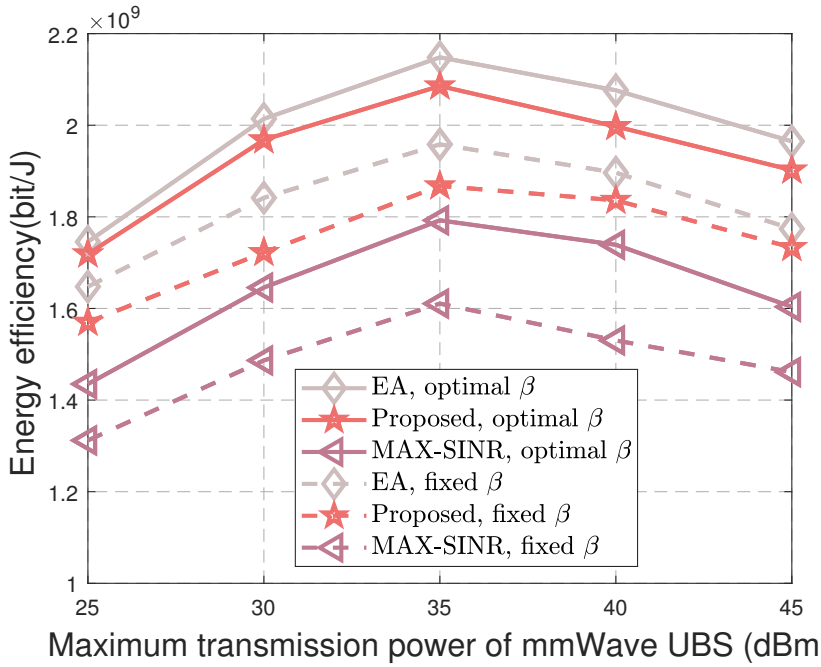

Figure 8. The energy efficiency varies with the maximum transmission power of the mmWave UBS.

Figure 9 demonstrates the impact of UE QoS rate requirements on energy efficiency. The figure indicates that energy efficiency decreases as the QoS rate requirement increases. This reduction occurs because, when the QoS rate requirement is excessively high, the network may fails to meet the QoS requirements for all UEs. As a result, some UEs experience transmission interruptions, leading to a decline in energy efficiency. The proposed algorithm outperforms the maximum SINR algorithm. It achieves a performance gain of 13.5% at a QoS rate requirement of 50 Mbps and 13.82% at a QoS rate requirement of 300 Mbps.

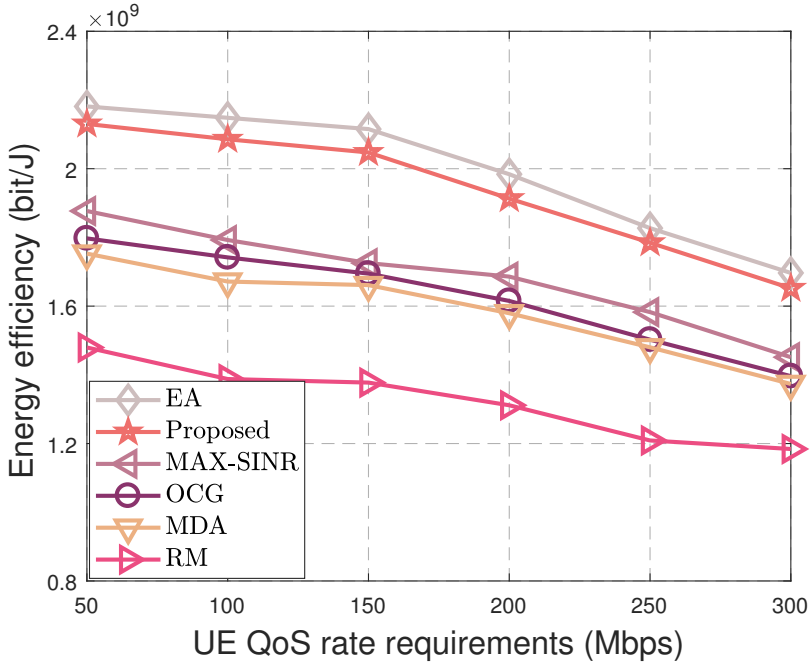

Figure 9. The energy efficiency varies with the UE QoS rate requirements of the mmWave UBS.

6. Conclusions

Considering the QoS rate requirement of the UEs, a cell-free user association, backhaul bandwidth allocation, and power allocation scheme is proposed to maximize the energy efficiency in mmWave networks. The optimization problem is a non-convex fractional programming problem, which is difficult to solve directly. Therefore, the original problem is first decoupled into three independent subproblems for alternating an iterative optimization solution. First, the non-convex subtractive power allocation subproblem is solved by transforming it into a convex problem using successive convex approximation and the Dinkelbach method. Second, a user association scheme based on energy efficiency maximization is proposed using the Lagrangian method. Finally, the formula derives a closed-form expression for the bandwidth allocation factor. Simulation results indicate that the proposed scheme improves system energy efficiency by at least 12.35% compared with other benchmark methods. This enhancement is achieved across various scenarios, including different beamwidths, cell-free cooperative UBS cluster size, densities of UBSs and UEs, transmission power, and UE QoS requirements. The proposed algorithm achieves performance close to EA while significantly reducing computational complexity, making it scalable for large-scale ultra-dense networks. These results highlight the effectiveness of the proposed method in enhancing energy efficiency and ensuring practical applicability in real-world scenarios, including disaster response and communication demands in mmWave networks.

Author Contributions: Conceptualization, Z.S., Q.L. and Z.J.; data curation, investigation, methodology, resources, and software, Z.S.; formal analysis and supervision, K.Z., J.Z. and X.S.; visualization and writing—original draft, Z.S., K.Z. and P.C.; validation and writing—review and editing, Z.S., Z.J. and P.C. All authors have read and agreed to the published version of the manuscript.

Funding: This research was supported by the National Key R&D Program of China under Grant 2024YFE0200102.

Institutional Review Board Statement: Not applicable.

Informed Consent Statement: Not applicable.

Data Availability Statement: The original contributions presented in this study are included in the article. Further inquiries can be directed to the corresponding author.

Conflicts of Interest: The authors declare no conflicts of interest.

Abbreviations

The definition of abbreviations:

Abbreviation	Definition
6G	sixth generation
AWGN	additive white Gaussian noise
BS	base station
CPU	central processing unit
FBC-HARQ-IR	finite blocklength coding, hybrid automatic repeat request with incremental redundancy
HAPS	high-altitude platform Station.
LoS	line-of-sight
KKT	Karush–Kuhn–Tucker
m-MIMO	massive multiple-input multiple-output
mmWave	millimeter-wave
NLoS	non-line-of-sight
QoS	quality of service
SCA	successive convex approximation
SINR	signal-to-interference-plus-noise ratio
SMBS	super macro base station
UAV	unmanned aerial vehicle
UBS	unmanned aerial vehicle base station
UE	user equipment

References

1. 3GPP Technical Report(TR) 22.829. Enhancement for Unmanned Aerial Vehicles (UAVs) (3GPP TR 22.829 Version 17.1.0 Release 17). September 2019. pp. 6–35. Available online: https://portal.3gpp.org/desktopmodules/Specifications/SpecificationDetails.aspx?specificationId=3557 (accessed on 19 January 2025).
2. Geraci, G.; Garcia-Rodriguez, A.; Azari, M.M.; Lozano, A.; Mezzavilla, M.; Chatzinotas, S.; Chen, Y.; Rangan, S.; Renzo, M.D. What Will the Future of UAV Cellular Communications Be? A Flight From 5G to 6G. *IEEE Commun. Surveys Tuts.* **2022**, *24*, 1304–1335. [CrossRef]
3. Xiao, Z.; Zhu, L.; Liu, Y.; Yi, P.; Zhang, R.; Xia, X. A survey on millimeter-wave beamforming enabled UAV communications and networking. *IEEE Commun. Surveys Tuts.* **2022**, *24*, 557–610. [CrossRef]
4. Zhu, L.; Zhang, J.; Xiao, Z.; Xia, X.-G.; Zhang, R. Multi-UAV aided millimeter-wave networks: Positioning clustering and beamforming. *IEEE Trans. Wire. Commun.* **2022**, *21*, 4637–4653. [CrossRef]
5. Erdelj, M.; Natalizio, E.; Chowdhury, K.R.; Akyildiz, I.F. Help from the Sky: Leveraging UAVs for Disaster Management. *IEEE Per. Comput.* **2017**, *16*, 24–32. [CrossRef]
6. Zhao, N.; Lu, W.; Sheng, M.; Chen, Y.; Tang, J.; Yu, F.R.; Wong, K. UAV-Assisted Emergency Networks in Disasters. *IEEE Wire. Commun.* **2019**, *26*, 45–51. [CrossRef]
7. Alsabah, M.; Naser, M.A.; Mahmmod, B.M.; Abdulhussain, S.H.; Eissa, M.R.; Al-Baidhani, A. 6G Wireless Communications Networks: A Comprehensive Survey. *IEEE Access* **2021**, 48191–148243. [CrossRef]
8. Hashmi, U.S.; Zaidi, S.A.R.; Imran, A.; Abu-Dayya, A. Enhancing Downlink QoS and Energy Efficiency Through a User-Centric Stienen Cell Architecture for mmWave Networks. *IEEE Trans. Green Commun. Net.* **2020**, *4*, 387–403. [CrossRef]
9. Yang, B.; Taleb, T.; Shen, Y.; Jiang, X.; Yang, W. Performance, Fairness, and Tradeoff in UAV Swarm Underlaid mmWave Cellular Networks with Directional Antennas. *IEEE Trans. Wire. Commun.* **2021**, *20*, 2383–2397. [CrossRef]
10. Alonzo, M.; Buzzi, S. Cell-Free and User-Centric Massive MIMO at Millimeter Wave Frequencies. In Proceedings of the 2017 IEEE 28th Annual International Symposium on Personal, Indoor, and Mobile Radio Communications (PIMRC), Montreal, QC, Canada, 8–13 October 2017; pp. 1–5.
11. Alavicheh, R.G.; Razavizadeh, S.M.; Yanikomeroglu, H. Integrated Access and Backhaul (IAB) in Low Altitude Platforms. *IEEE Open J. Commun. Soc.* **2024**, *5*, 5890–5904. [CrossRef]

12. Jazi, A.H.; Razavizadeh, S.M.; Svensson, T. Integrated Access and Backhaul (IAB) in Cell-Free Massive MIMO Systems. *IEEE Access* **2023**, *11*, 71658–71667. [CrossRef]
13. Shafie, R.; Omidi, M.J.; Abbasi, O.; Yanikomeroglu, H. MIMO-NOMA Enabled Sectorized Cylindrical Massive Antenna Array for HAPS with Spatially Correlated Channels. *IEEE Trans. Wire. Commun.* **2024**, *23*, 15155–15168. [CrossRef]
14. Kurt, G.K.; Khoshkholgh, M.G.; Alfattani, S.; Ibrahim, A.; Darwish, T.S.J.; Alam, M.S. A Vision and Framework for the High Altitude Platform Station (HAPS) Networks of the Future. *IEEE Commun. Surveys Tuts.* **2021**, *23*, 729–779. [CrossRef]
15. Song, T.; Lopez, D.; Meo, M.; Piovesan, N.; Renga, D. High Altitude Platform Stations: The New Network Energy Efficiency Enabler in the 6G Era. In Proceedings of the 2024 IEEE Wireless Communications and Networking Conference (WCNC), Dubai, United Arab Emirates, 21–24 April 2024; pp. 1–6.
16. He, Y.; Shen, M.; Zeng, F.; Zheng, H.; Wang, R.; Zhang, M.; Liu, X. Energy Efficient Power Allocation for Cell-Free mmWave Massive MIMO with Hybrid Precoder. *IEEE Commun. Lett.* **2022**, *26*, 394–398. [CrossRef]
17. Wang, J.; Wang, B.; Fang, J.; Li, H. Millimeter Wave Cell-Free Massive MIMO Systems: Joint Beamforming and AP-User Association. *IEEE Wire. Commun. Lett.* **2022**, *11*, 298–302. [CrossRef]
18. Wang, Z.; Li, M.; Liu, R.; Liu, Q. Joint User Association and Hybrid Beamforming Designs for Cell-Free mmWave MIMO Communications. *IEEE Trans. Commun.* **2022**, *70*, 7307–7321. [CrossRef]
19. Hao, C.; Vu, T.T.; Ngo, H.Q.; Dao, M.N.; Dang, X.; Wang, C.; Matthaiou, M. Joint User Association and Power Control for Cell-Free Massive MIMO. *IEEE Internet Things J.* **2024**, *11*, 15823–15841. [CrossRef]
20. Lin, Z.; Niu, H.; An, K.; Wang, Y.; Zheng, G.; Chatzinotas, S.; Hu, Y. Refracting RIS Aided Hybrid Satellite-Terrestrial Relay Networks: Joint Beamforming Design and Optimization. *IEEE Trans. Aerosp. Electron. Syst.* **2022**, *58*, 3717–3724. [CrossRef]
21. Lin, Z.; Niu, H.; He, Y.; An, K.; Zhong, X.; Chu, Z.; Xiao, P. Self-Powered Absorptive Reconfigurable Intelligent Surfaces for Securing Satellite-Terrestrial Integrated Networks. *China Commun.* **2024**, *21*, 276–291.
22. Abbasi, O.; Yanikomeroglu, H. A Cell-Free Scheme for UAV Base Stations with HAPS-Assisted Backhauling in Terahertz Band. In Proceedings of the ICC 2022—IEEE International Conference on Communications, Seoul, Republic of Korea, 16–20 May 2022; pp. 249–254.
23. Abbasi, O.; Yanikomeroglu, H. UxNB-Enabled Cell-Free Massive MIMO with HAPS-Assisted Sub-THz Backhauling. *IEEE Trans. Veh. Technol.* **2024**, *73*, 6937–6953. [CrossRef]
24. Zhao, J.; Hu, F.; Gong, Y.; Wang, D. Downlink Resource Intelligent Scheduling in mmWave Cell-Free Urban Vehicle Network. *IEEE Trans. Veh. Tech.* **2024**, *73*, 15525–15537. [CrossRef]
25. Ammar, H.A.; Adve, R.; Shahbazpanahi, S.; Boudreau, G.; Srinivas, K.V. User-Centric Cell-Free Massive MIMO Networks: A Survey of Opportunities, Challenges and Solutions. *IEEE Commun. Surveys Tuts.* **2022**, *24*, 611–652. [CrossRef]
26. Lee, H.; Park, J.; Lee, S.H.; Lee, I. Message-Passing Based User Association and Bandwidth Allocation in HetNets with Wireless Backhaul. *IEEE Trans. Wire. Commun.* **2024**, *22*, 704–717. [CrossRef]
27. Dong, S.; Zhan, J.; Hu, W.; Mohajer, A.; Bavaghar, M.; Mirzaei, A. Energy-Efficient Hierarchical Resource Allocation in Uplink-Downlink Decoupled Noma Hetnets. *IEEE Trans. Net. Serv. Man.* **2023**, *20*, 3380–3395. [CrossRef]
28. Yu, X.; Huang, X.; Wang, K.; Shu, F.; Dang, X. Joint Design of Power Allocation, Beamforming, and Positioning for Energy-Efficient UAV-Aided Multiuser Millimeter-Wave Systems. *IEEE J.S. Areas Commun.* **2022**, *40*, 2930–2945. [CrossRef]
29. Lin, Z.; Lin, M.; Champagne, B.; Zhu, W.-P.; Al-Dhahir, N. Secrecy-Energy Efficient Hybrid Beamforming for Satellite-Terrestrial Integrated Networks. *IEEE Trans. Commun.* **2021**, *69*, 6345–6360. [CrossRef]
30. Lin, Z.; An, K.; Niu, H.; Hu, Y.; Chatzinotas, S.; Zheng, G.; Wang, J. SLNR-Based Secure Energy Efficient Beamforming in Multibeam Satellite Systems. *IEEE Trans. Aerosp. Electron. Syst.* **2023**, *59*, 2085–2088. [CrossRef]
31. Zhang, X.; Wang, J.; Poor, H.V. Statistical Delay and Error-Rate Bounded QoS Provisioning Over mmWave Cell-Free M-MIMO and FBC-HARQ-IR Based 6G Wireless Networks. *IEEE J. S. Areas Commun.* **2020**, *38*, 1661–1677. [CrossRef]
32. Mai, T.C.; Ngo, H.Q.; Tran, L.-N. Energy Efficiency Maximization in Large-Scale Cell-Free Massive MIMO: A Projected Gradient Approach. IEEE Trans. *Wire. Commun.* **2022**, *21*, 6357–6371. [CrossRef]
33. Vu, T.X.; Chatzinotas, S.; ShahbazPanahi, S.; Ottersten, B. Joint Power Allocation and Access Point Selection for Cell-free Massive MIMO. In Proceedings of the ICC 2020—2020 IEEE International Conference on Communications (ICC), Dublin, Ireland, 7–11 June 2020; pp. 1–6.
34. Guo, F.; Lu, H.; Gu, Z. Joint Power and User Grouping Optimization in Cell-Free Massive MIMO Systems. *IEEE Trans. Wire. Commun.* **2022**, *21*, 991–1006. [CrossRef]
35. Alam, M.S.; Kurt, G.K.; Yanikomeroglu, H.; Zhu, P.; Dao, N.D. High Altitude Platform Station Based Super Macro Base Station Constellations. *IEEE Commun. Mag.* **2021**, *59*, 103–109. [CrossRef]
36. Xiao, Z.; He, T.; Xia, P.; Xia, X.-G. Hierarchical Codebook Design for Beamforming Training in Millimeter-wave Communication. *IEEE Trans. Wire. Commun.* **2016**, *15*, 3380–3392. [CrossRef]
37. Shokri-Ghadikolaei, H.; Fischione, C.; Fodor, G.; Popovski, P.; Zorzi, M. Millimeter Wave Cellular Networks: A MAC Layer Perspective. *IEEE Trans. Commun.* **2015**, *63*, 3437–3458. [CrossRef]

38. Demir, Ö.T.; Björnson, E.; Sanguinetti, L. Foundations of User-Centric Cell-Free Massive MIMO. *Found. Trends® Signal Process.* **2021**, *14*, 162–472. [CrossRef]
39. Rahman, A.B.; Chen, Y.S.; Tsiropoulou, E.E.; Papavassiliou, S. SynergyWave: Bandwidth Splitting and Power Control in Integrated Access and Backhaul Networks. In Proceedings of the ICC 2024—IEEE International Conference on Communications, Denver, CO, USA, 9–13 June 2024; pp. 31–36.
40. Liu, H.; Zhang, H.; Cheng, J.; Leung, V.C.M. Energy Efficient Power Allocation and Backhaul Design in Heterogeneous Small Cell Networks. In Proceedings of the 2016 IEEE International Conference on Communications (ICC), Kuala Lumpur, Malaysia, 22–27 May 2016; pp. 1–5.
41. Zhang, H.; Liu, H.; Cheng, J.; Leung, V.C.M. Downlink Energy Efficiency of Power Allocation and Wireless Backhaul Bandwidth Allocation in Heterogeneous Small Cell Networks. *IEEE Trans. Commun.* **2018**, *66*, 1705–1716. [CrossRef]
42. Zappone, A.; Björnson, E.; Sanguinetti, L.; Jorswieck, E. Globally Optimal Energy-Efficient Power Control and Receiver Design in Wireless Networks. *IEEE Trans. Signal Process* **2017**, *65*, 2844–2859. [CrossRef]
43. Dinkelbach, W. On Nonlinear Fraction Programming. *Manage. Sci.* **1967**, *13*, 492–498. [CrossRef]
44. Yu, X.; Wang, G.; Huang, X.; Wang, K.; Xu, W.; Rui, Y. Energy Efficient Resource Allocation for Uplink RIS-Aided Millimeter-Wave Networks with NOMA. *IEEE Trans. Mobile Comput.* **2024**, *23*, 423–436. [CrossRef]
45. Boyd, S.; Vandenberghe, L. *Convex Optimization*; Cambridge University Press: Cambridge, UK, 2004; ISBN 9780521833783.
46. Kim, S.-J.; Koh, K.; Lustig, M.; Boyd, S.; Gorinevsky, D. An Interior-Point Method for Large-Scale ℓ_1-Regularized Least Squares. *IEEE J. Sel. Topics Signal Process* **2007**, *1*, 606–617. [CrossRef]
47. Yi, X.; Li, X.; Xie, L.; Johansson, K.H. Distributed Online Convex Optimization with Time-Varying Coupled Inequality Constraints. *IEEE Trans. Signal Process* **2020**, *68*, 731–746. [CrossRef]
48. Lou, Z.; Belmekki, B.E.Y.; Alouini, M.-S. HAPS in the Non-Terrestrial Network Nexus: Prospective Architectures and Performance Insights. *IEEE Wire. Commun.* **2023**, *30*, 52–58. [CrossRef]
49. Suganuma, S.; Nguyen, D.H.; Nishioka, Y.; Shimamura, K.; Mori, K.; Yokota, S. The Logistics System by Rotary Wing Unmanned Aerial Vehicle with 28GHz Microwave Power Transmission. In Proceedings of the 2019 IEEE Wireless Power Transfer Conference (WPTC), London, UK, 18–21 June 2019; pp. 413–416.
50. 3GPP Technical Report(TR)38.913. 5G, Study on Scenarios and Requirements for Next Generation Access Technologies (3GPP TR 38.913 Version 16.0.0 Release 16). July 2020. pp. 9–21. Available online: https://portal.3gpp.org/desktopmodules/Specifications/SpecificationDetails.aspx?specificationId=2996 (accessed on 19 January 2025).
51. Liu, C.-H.; Ho, K.-H.; Wu, J.-Y. Mmwave UAV Networks with Multi-Cell Association: Performance Limit and Optimization. *IEEE J. Sel. Areas Commun.* **2019**, *37*, 2814–2831. [CrossRef]
52. Björnson, E.; Hoydis, J.; Sanguinetti, L. Massive MIMO Networks: Spectral, Energy, and Hardware Efficiency. *Found. Trends® Signal Process.* **2017**, *11*, 154–655. [CrossRef]
53. Zhao, J.; Gao, F.; Kuang, L.; Wu, Q.; Jia, W. Channel Tracking with Flight Control System for UAV mmWave MIMO Communications. *IEEE Commun. Lett.* **2018**, *22*, 1224–1227. [CrossRef]